Protein Science (1994), *3*:103–108. Cambridge University Press. Printed in the USA.
Copyright © 1994 The Protein Society

Kinetics and thermodynamics of thermal denaturation in acyl carrier protein

L.A. HORVATH, J.M. STURTEVANT, AND J.H. PRESTEGARD
Department of Chemistry, Yale University, New Haven, Connecticut 06511

(RECEIVED May 13, 1993; ACCEPTED October 25, 1993)

Abstract

The denaturation of *Escherichia coli* acyl carrier protein (ACP) in buffers containing both monovalent and divalent cations was followed by variable-temperature NMR and differential scanning calorimetry. Both high concentrations of monovalent salts (Na^+) and moderate concentrations of divalent salts (Ca^{2+}) raise the denaturation temperature, but calorimetry indicates that a significant increase in the enthalpy of denaturation is obtained only with the addition of a divalent salt. NMR experiments in both low ionic strength monovalent buffers and low ionic strength monovalent buffers containing calcium ions show exchange between native and denatured forms to be slow on the NMR time scale. However, in high ionic strength monovalent buffers, where the temperature of denaturation is elevated as it is in the presence of Ca^{2+}, the transition is fast on the NMR time scale. These results suggest that monovalent and divalent cations may act to stabilize ACP in different ways. Monovalent ions may nonspecifically balance the intrinsic negative charge of this protein in a way that is similar for native, denatured, and intermediate forms. Divalent cations provide stability by binding to specific sites present only in the native state.

Keywords: acyl carrier protein; DSC; NMR; protein denaturation

Proteins typically function under conditions of rather marginal stability with only a few kilocalories per mole separating native states from denatured states (Privalov & Gill, 1988). Yet, proteins are generally considered to exist in discrete states in which native, folded forms are easily distinguished from their unfolded counterparts. There is actually considerable experimental evidence that leads to this picture. NMR studies conducted near denaturation midpoints, for example, usually show discrete pairs of resonances that belong to folded and unfolded forms exchanging on a time scale that is slow compared to the inverse frequency separation of the resonances (10^{-2} s) (Roder, 1989). We might, however, expect a range of behaviors, particularly in proteins that are small, lack disulfide bonds, or are destabilized by local charge imbalance.

Acyl carrier protein (ACP) is a protein that might be expected to depart from simple denaturation behavior. *Escherichia coli* ACP is small (8,847 Da), has an excess of 16 negatively charged amino acids, and has no stabilizing disulfide bonds (Prescott & Vagelos, 1972). In addition, its role as a carrier of the growing acyl chain during fatty acid biosynthesis requires ACP to interact with at least 6 different enzymes involved in the synthesis cycle. This functional diversity may require more than normal conformational flexibility.

Reprint requests to: J.H. Prestegard, Department of Chemistry, Yale University, New Haven, Connecticut 06511.

The 3-dimensional structure of *E. coli* ACP was determined using NMR methods in 1987 (Holak et al., 1987). Although the qualitative appearance of the spectra was that of a protein with a single well-defined structure, the structures generated by pseudoenergy and distance geometry calculations were of poor resolution. This led to speculation that multiple protein forms exist in rapid equilibrium even under conditions where the protein appears to be largely folded (Kim & Prestegard, 1989, 1990).

Here we examine the thermodynamic and kinetic behavior of *E. coli* ACP during thermal denaturation using differential scanning calorimetry and high-resolution ^1H NMR. The calorimetry data under low ionic strength conditions are consistent with a simple 2-state denaturation. Under conditions that include high concentrations of monovalent salts, however, the NMR data do show rapid interconversion between native and denatured forms of ACP. The calorimetry data obtained under these conditions also show some degree of departure from simple 2-state denaturation.

The rate of interconversion, as well as thermodynamic parameters relating native and denatured states, are shown to depend on environmental factors such as ionic strength and the presence of divalent metal ions. ACP has been shown to possess divalent ion binding sites (Shulz, 1977; Frederick et al., 1988; Tener & Mayo, 1989). Ions in these sites may play structural roles that are necessary for the function of the protein. Analysis of NMR spectra and calorimetry data under high and low ionic strength conditions, and in the presence of Ca^{2+}, can lead

to a quantitative assessment of exchange rates and to some insight into factors that stabilize the native structure of ACP.

Results

Calorimetry

Interpretations of differential scanning calorimetry (DSC) data are usually made by using the equilibrium expression

$$\left(\frac{\partial \ln K}{\partial T}\right)_P = \frac{\Delta H_{vH}}{RT^2}, \quad (1)$$

where ΔH_{vH} is the van't Hoff enthalpy, a standard-state quantity generally comparable to the true calorimetric enthalpy ΔH_{cal}. After subtracting the appropriate baseline, the data can be analyzed using a least-squares fit procedure based on a 2-state denaturation model (Sturtevant, 1987). The equilibrium of interest is the denaturation of ACP:

$$ACP_N \rightleftharpoons ACP_D.$$

Using α to indicate the extent of denaturation, it is possible to substitute $K = \alpha/(1-\alpha)$ into Equation 1. After taking the derivative and using $c_{ex} = \Delta h_{cal}(\partial\alpha/\partial T)$, where Δh_{cal} is ΔH_{cal} divided by the molecular weight of the protein, we arrive at the following expression for the excess specific heat:

$$c_{ex} = \alpha(1-\alpha)\beta \frac{\Delta h_{cal}^2}{RT^2} \quad (2)$$

(Connelly et al., 1991). Using a nonlinear least-squares curve fitting procedure, values for Δh_{cal}, β, and $T_{1/2}$, the temperature at the midpoint of denaturation, are obtained. In Equation 2 the value $\beta = \Delta H_{vH}/\Delta h_{cal}$ provides a test of whether or not the denaturation is a simple 2-state process. For a pure 2-state transition, β should be equal to the molecular weight of the protein.

Figure 1 shows typical DSC curves observed for ACP in low ionic strength monovalent buffer in the absence (A) and presence (B) of Ca^{2+}. Calcium levels in the data shown are 8.3 mM, or approximately 6 equivalents per mole of protein. It is believed that there are 2 well-defined Ca^{2+} binding sites in the native protein (Frederick et al., 1988). However, the binding constants for these sites are relatively weak (Tener & Mayo, 1989), and calorimetry shows pronounced changes with Ca^{2+} concentrations until at least 4 equivalents have been added. The solid curves in Figure 1 represent the observed data, and the dashed curves represent the calculated best fit and the calculated chemical baseline. The parameters evaluated by curve fitting are listed in Table 1. Because of the asymmetry introduced by the sloping pre- and posttransition baselines, the temperatures listed in the table differ somewhat from the apparent midpoint temperatures seen in Figure 1: 55 °C for ACP in low ionic strength buffer and 67.2 °C for ACP in low ionic strength buffer with Ca^{2+} added. As is to be expected for a small protein, the transitions are rather broad, especially in the absence of Ca^{2+}. The enthalpy observed in the absence of Ca^{2+}, 4.3 cal g^{-1}, is close to the average figure for globular proteins. The value, 7.2 cal g^{-1}, observed in the presence of Ca^{2+} is substantially larger. In fact, it is near the maximum of the range thought typical of globular proteins (Privalov, 1980).

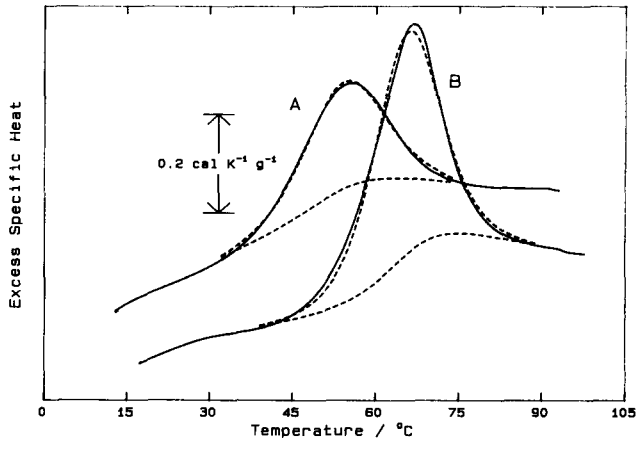

Fig. 1. DSC traces, after subtraction of the instrumental baseline, obtained with ACP at a concentration of 12.3 mg mL^{-1} in low ionic strength buffer. Curve A: No Ca^{2+} present. Curve B: In the presence of 6 equivalents of Ca^{2+}. In each case the solid curve represents the observed data and the dashed curves are the best fit curve and the calculated chemical baseline.

The 12 °C increase in $T_{1/2}$ caused by the addition of Ca^{2+} indicates a pronounced stabilization of the native state of the protein relative to the denatured state in the presence of Ca^{2+}. Heat capacity data of improved reliability will have to be obtained before quantitative conclusions can be drawn from the apparently large increase in the enthalpy of unfolding upon the addition of Ca^{2+}, 25 kcal mol^{-1}, and the correspondingly large increase in the entropy of unfolding, 75 cal K^{-1} mol^{-1}. The approximate agreement between H_{cal} and H_{vH} indicates that the unfolding process is 2-state, or nearly so, both in the absence and in the presence of Ca^{2+}.

Table 1. *Thermodynamic parameters for the thermal denaturation of ACP at pH 6.1*[a]

Buffer conditions	$T_{1/2}$ (°C)	Δh_{cal} (cal/g)	ΔH_{cal} (kcal/mol)	ΔH_{vH} (kcal/mol)	ΔC_p (kcal/K mol)	SD (% of $C_{ex,max}$)
Low salt	52.7	4.34	38.3	40.8	0.80	1.3
Low salt, Ca^{2+}	64.3	7.18	63.5	55.3	1.54	2.0
High salt	63.2	4.23	37.4	47.6	0.67	0.9

[a] Estimated uncertainties: $T_{1/2}$, ±0.2 °C; ΔH_{cal}, ±10%; ΔC_p, ±20%.

One might anticipate similar stabilization of the native state by addition of large amounts of monovalent salts. ACP is a highly negatively charged protein with substantial potential for charge–charge repulsion in the native state. In fact, such similarities in stabilization by monovalent and divalent ions were suggested some time ago (Shulz, 1977). Examination of denaturation behavior in the presence of higher concentrations of monovalent salts is also of some relevance, because NMR data used in the structural determination of this protein were obtained from samples containing rather high concentrations of monovalent cations (10 mM ACP in approximately 250 mM KH_2PO_4 buffer [Holak et al., 1987]).

Figure 2 shows DSC curves observed for ACP in low ionic strength monovalent buffer (A, 50 mM sodium acetate) and high ionic strength monovalent buffer (C, 240 mM sodium acetate). At higher concentrations of monovalent salt, the $T_{1/2}$ increased to 63 °C, much as seen in response to the addition of Ca^{2+}. However, the enthalpy of denaturation showed no significant change. Thus, the increase in denaturation temperature must be primarily associated with a decrease in the entropy of denaturation in the presence of high concentrations of monovalent ions. The value of β was also slightly higher than the molecular weight of the protein. A possible explanation of this behavior is dimerization or aggregation in the denatured state at higher salt concentrations. At higher protein concentrations in the high ionic strength monovalent buffer (data not shown) β increased further, as would be expected if some aggregation occurred. Thus, while both monovalent and divalent salts raise denaturation temperatures, the mechanisms are quite different. There is also some departure from ideal behavior in the presence of high concentrations of monovalent salts.

NMR

One might expect that differences in stabilization mechanisms would also be seen in the rates of exchange between native and denatured states. NMR provides a useful probe of these kinetic processes. When exchange is slow on the NMR time scale and separate peaks are seen for the species in equilibrium, broadening of a resonance can be used to calculate the lifetime of a proton in a particular state using the equation

$$\Delta\Delta\nu = \frac{1}{\pi\tau}. \tag{3}$$

Here $\Delta\Delta\nu$ is the increase in line width at half height due to exchange and τ is the lifetime of a spin in a given state. When the line observed belongs to the native state, the inverse of τ is the rate of denaturation, k_1.

Figure 3 shows the aromatic region from a series of NMR spectra collected from a 2.9 mM ACP sample in 48 mM sodium acetate buffer, pH 6.3 (low ionic strength). The spectrum at 30 °C corresponds to the native structure. The resonances are assigned as follows: a, His-75 ϵ; b, Phe-50 δ; c, Phe-50 $\epsilon\xi$; d, Phe-28 $\delta\epsilon$; e, Tyr-71 δ; f, Phe-28 ξ; g, Tyr-71 ϵ. As the temperature is raised, there are obviously temperature-dependent shifts of all resonances. However, we also note the appearance of a second set of resonances beginning at 40 °C. These grow at the expense of the initial native state resonances, until they dominate the spectrum at 65 °C. Thus, ACP under low ionic strength conditions exists in a slow exchange equilibrium in which native and denatured states give rise to discrete proton resonances. The midpoint in the denaturation occurs at approximately the same temperature as in the DSC trace for a sample at similar ionic strength, and the range of denaturation is similar to that

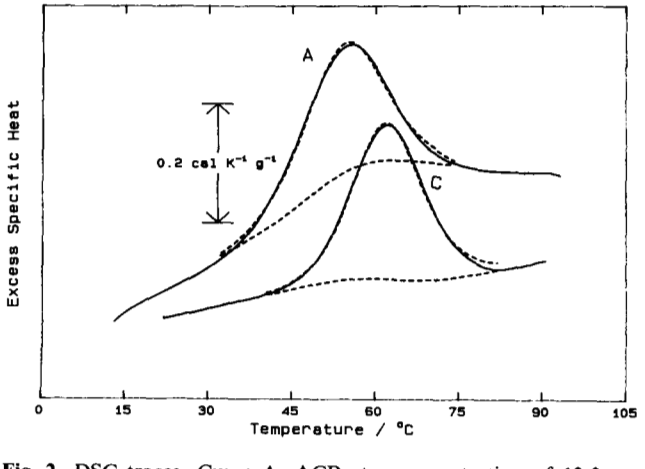

Fig. 2. DSC traces. Curve A: ACP at a concentration of 12.3 mg mL^{-1} in low ionic strength monovalent buffer. Curve C: ACP at a concentration of 7.15 mg mL^{-1} in high ionic strength monovalent buffer.

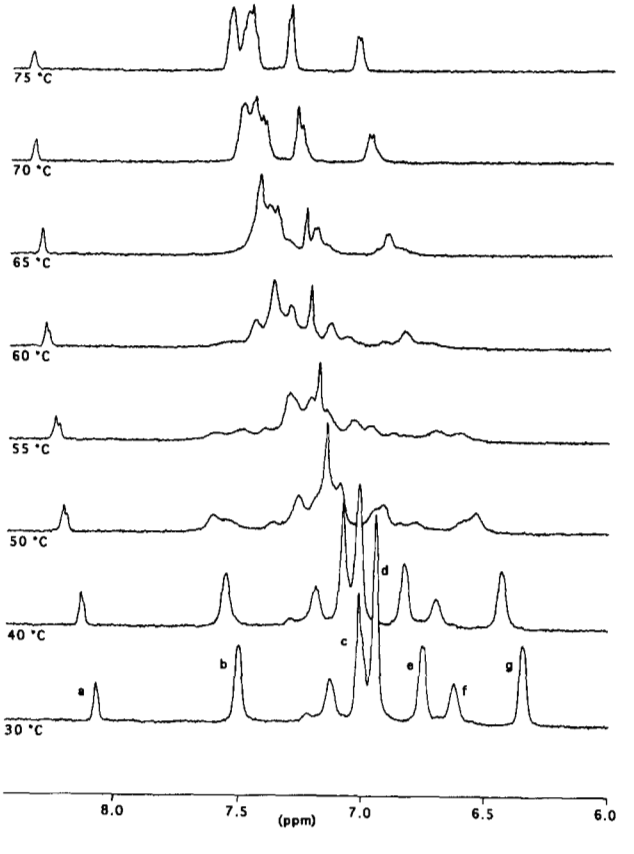

Fig. 3. Spectra of 2.9 mM *E. coli* ACP in 48 mM deuterated sodium acetate buffer, pH 6.3. Resonances are assigned as follows: a, His-75 ϵ; b, Phe-50 δ; c, Phe-50 $\epsilon\xi$; d, Phe-28 $\delta\epsilon$; e, Tyr-71 δ; f, Phe-28 ξ; g, Tyr-71 ϵ.

observed in the calorimetry experiments. Considerable line broadening near the midpoint of denaturation (55 °C) indicates that the exchange rate may be near the NMR time scale.

The 55 °C spectrum, which is near the midpoint of denaturation, gives the clearest indication of the exchange rate. Pairs of distinct peaks for both the Tyr-71 δ and ϵ protons and the Phe-50 δ protons are most easily observed. Using an average non-exchange line width derived from the 30 °C and 75 °C spectra, the exchange contribution to the line width for each of these states can be estimated and an average rate at 55 °C calculated. The rate, k_1, is 54 ± 3 s^{-1}.

When calcium is added to the low ionic strength ACP sample, the midpoint of denaturation is significantly increased (Fig. 4). This increase is nearly equivalent to that seen in the calorimetric data. Each resonance in the aromatic region again evolves into 2 quite distinct peaks, indicating that the exchange rate for a low ionic strength sample containing Ca^{2+} is slow on the NMR time scale. Near the midpoint of the transition (65 °C), an average exchange rate of 6 ± 3 s^{-1} is found. It is noteworthy that even though the temperature of observation is higher, the absolute rate for denaturation at the transition midpoint is considerably less in the presence of calcium. Thus, for a given temperature, calcium stabilizes the native ACP structure and slows the rate of native to denatured exchange.

Spectra taken under high ionic strength conditions without the presence of divalent metal ions are shown in Figure 5. The mid-

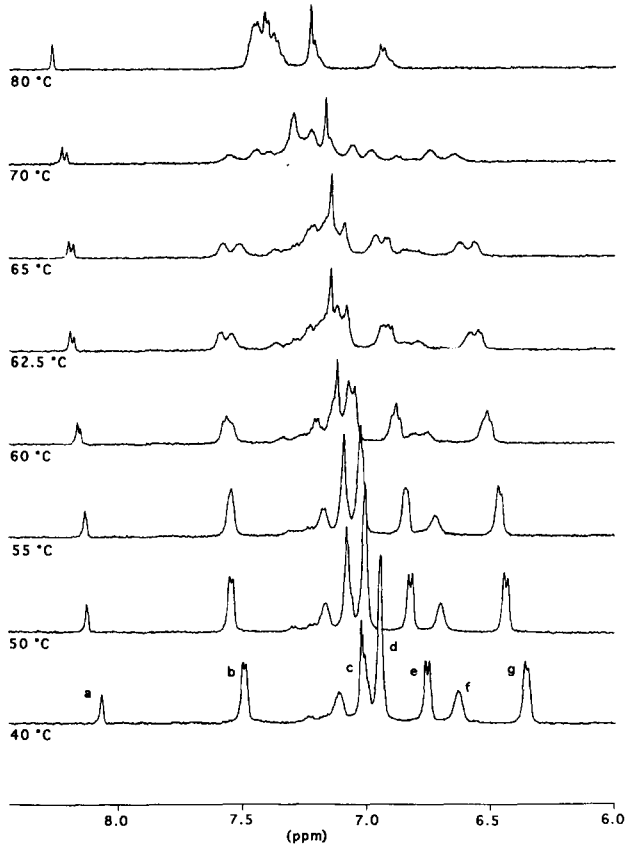

Fig. 4. Spectra of 2.9 mM *E. coli* ACP in 48 mM deuterated sodium acetate buffer, pH 6.3. Calcium chloride was added to a final concentration of 10 mM. Resonances are assigned as in Figure 3.

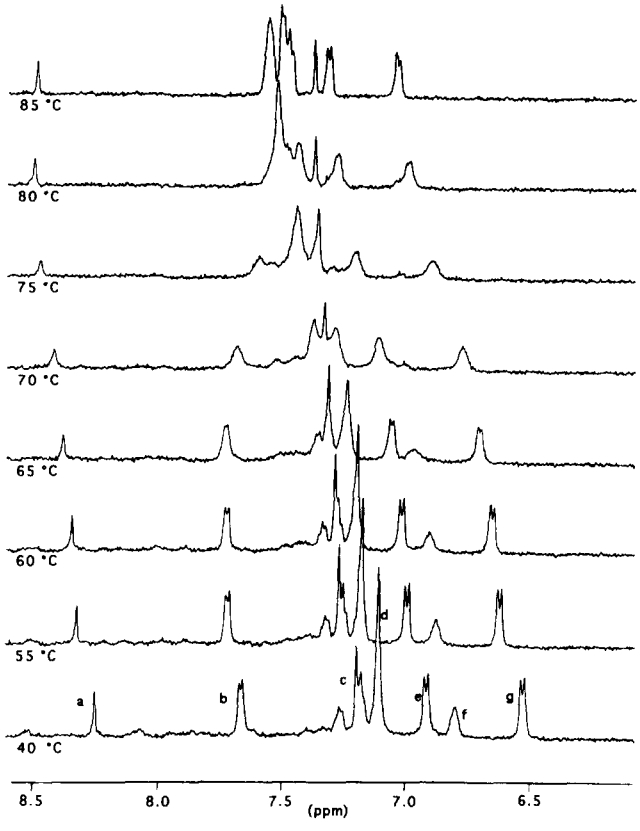

Fig. 5. Spectra of 3.9 mM *E. coli* ACP in 240 mM deuterated sodium acetate buffer, pH 6.15. Resonances are assigned as in Figure 3.

point of denaturation is increased to approximately 70 °C, an increase similar to that seen in the low ionic strength buffer on the addition of calcium. The Phe-50 δ and Tyr-71 δ and ϵ resonances of this sample remain as single peaks throughout the denaturation, indicating that the rate of exchange is now fast on the NMR time scale.

Fast exchange causes the appearance of a single peak at a position $\bar{\omega}$, where $\bar{\omega}$ is determined by the fraction of spins in the native and denatured forms at a particular temperature. The position of the averaged resonance $\bar{\omega}$ is given by

$$\bar{\omega} = f_N \omega_N + f_D \omega_D, \tag{4}$$

where f_N and f_D are the mole fractions of protein and ω_N and ω_D are the resonance positions in the native and denatured forms. Thus, one expects protein denaturation to cause abrupt changes in chemical shifts and line broadening.

Assuming that line broadening due to processes other than exchange varies continuously over the temperature range studied, it is possible to isolate exchange contributions to the line width for well-resolved resonances and use them to estimate the rate of exchange between the native and denatured forms of ACP. The appropriate expression is

$$\Delta\Delta\nu = \frac{f_D(1-f_D)(\omega_N-\omega_D)^2}{\pi\left[k_1 + k_1\dfrac{(1-f_D)}{f_D}\right]}. \tag{5}$$

In the above equation, k_1 is the rate of transition from the native to denatured state and $[k_1(1-f_D)]/f_D$ is the rate of the reverse transformation (Carrington & McLachlan, 1978).

According to Equation 5, the line broadening should be proportional to the change in chemical shift squared. Qualitatively the expected correlation is illustrated in Figures 6 and 7. Figure 6 shows the change in chemical shift with temperature. Note that some resonances are shifted upfield while others are shifted downfield. Equation 5 suggests that only the magnitude of these shifts is important. Figure 7 shows the change in line width with temperature, corrected for coupling and other line width contributions. Note that those resonances that shift the most – Phe-28 ξ, Tyr-71 ϵ, and Phe-50 δ – also experience the greatest broadening. Using Equation 5 and data from resonances that are well resolved and significantly broadened at the denaturation midpoint – Phe-50 δ, and Tyr-71 δ, and Tyr-71 ϵ – at 70 °C an average exchange rate of 3,580 ± 800 s^{-1} is calculated. This rate is considerably faster than the rate observed at a similar temperature in low ionic strength buffer with Ca^{2+} present. Thus, rates of ACP denaturation vary considerably with environmental conditions, and both fast and slow exchange conditions can be created for ACP denaturation. Although either Ca^{2+} or high concentrations of monovalent ions can stabilize ACP to similar extents, their effects on the rate of denaturation are quite different.

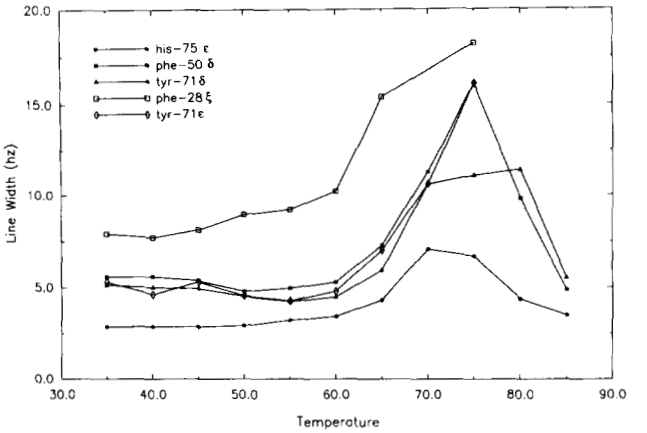

Fig. 7. Dependence of line width on temperature for 5 well-resolved resonances from the NMR spectra of ACP. Line widths were obtained from a curve fitting program in which lines were fit using Lorentzian lines separated by known coupling constants. Line widths and intensities were varied using a simulated annealing algorithm to optimize fits.

Discussion

The observation that divalent ions and monovalent ions behave in a qualitatively different manner when stabilizing ACP may provide some insight into the nature of counter ion interactions within the protein. Monovalent ions may well be displaying a rather nonspecific interaction related to the tendency to collect positively charged counter ions in regions surrounding this negatively charged protein. The observation that the enthalpy of protein denaturation changes little with the addition of monovalent salt indicates that monovalent ions may stabilize the folded form and the denatured form of the protein to a similar degree. It would seem reasonable that any transition state between native and denatured forms would also be stabilized to a similar degree, and these factors would contribute little if anything to a change in an activation energy for denaturation. The increase in the denaturation rate at the transition midpoint upon the addition of monovalent ions would therefore be largely a consequence of the transition occurring at a higher temperature.

Divalent ions, on the other hand, are likely to be bound to specific structural sites that are present only in the native state. This would explain the large increase in enthalpy of denaturation. While we cannot absolutely rule out the possibility that the increase in ΔH is the result of further destabilization of the unfolded form, we point out that the NMR spectra for unfolded forms in the presence of Ca^{2+} and low levels of Na^+ are virtually identical (compare spectra at 70 °C in Fig. 3 and 80 °C in Fig. 4).

It is also likely that specific ion binding sites will be disrupted in the very early stages of denaturation. The fully folded form will, therefore, be stabilized relative to structures near the maximum energy point in the denaturation pathway. Activation energies would increase and denaturation rates would be lower at comparable denaturation temperatures.

Our observations, therefore, support a specific structural role for divalent ions in ACP. The denaturation behavior in the presence of these ions is near ideal, and shows more typical slow exchange between native and denatured states. This behavior suggests improved conditions for NMR-based structural work. Although the general locality of divalent ion binding sites in ACP has been identified by NMR studies (Frederick et al., 1988), a complete redetermination of ACP structure in the presence of divalent cations has not as yet been accomplished. Denaturation behavior in the presence of high levels of monovalent salts (conditions similar to those under which previous structural data were collected) shows both rapid exchange between states and some departure from 2-state denaturation. While this nonideality could result from aggregation in the denatured state, the lack of native state stabilization and rapid exchange between various states could have contributed to difficulties in previous NMR studies.

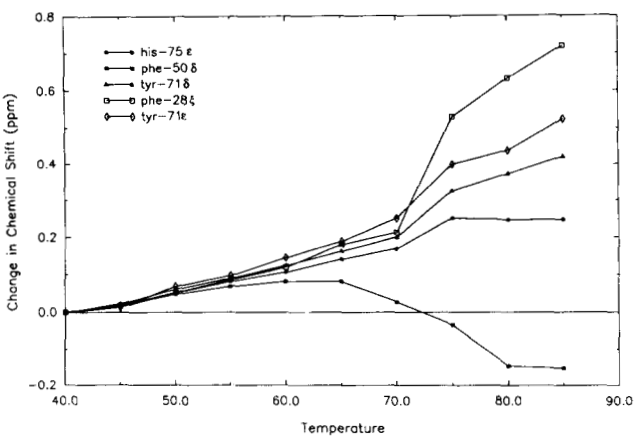

Fig. 6. Change of chemical shift with increasing temperature for 3.9 mM ACP in 240 mM deuterated sodium acetate buffer, pH 6.15. Chemical shifts were measured against an internal dioxane reference at 4.0 ppm.

Materials and methods

Protein purification

E. coli strain MgT7pLysS cells that had been transformed with the pET-3a vector containing the synthetic ACP gene under T7 promoter control were grown to high optical density in TB medium (Sambrook et al., 1989). Using a method developed by Hill (manuscript in prep.), ACP was purified from the cells. This purification is based on that given by Rock and Cronan (1980). However, instead of using homogenization to achieve cell lysis, the cells were first suspended in a 10 mM EDTA, 50 mM Tris buffer and then frozen and thawed 3 times. The cell suspension was then subjected to short periods of ultrasonication until the suspension was quite fluid. The 2-propanol precipitation given in the Rock and Cronan (1980) procedure was also replaced by a 60% saturated ammonium sulfate fractionation, and a Sepharose FF anion exchange column (Sigma) was used in place of the DEAE resin. Using the above cell line and the alternate purification scheme, it was possible to prepare approximately 100 mg of pure ACP from a 1-L growth in TB medium.

Calorimetry

ACP for use in the low ionic strength calorimetry experiment was dialyzed against a 50 mM sodium acetate, 0.5 mM DTT buffer, pH 6.1. The final protein concentration was 12.3 mg mL^{-1} (1.4 mM). In the experiments performed in the presence of Ca^{2+}, calcium chloride (final concentration 8.4 mM) was added to the low ionic strength ACP sample 15 min prior to scanning. ACP for use in the high ionic strength monovalent buffer experiment was dialyzed against 240 mM sodium acetate, 0.5 mM DTT buffer, pH 6.1. The final protein concentration was 7.15 mg mL^{-1} (1.6 mM). Two calorimeters, the MC-2 (Microcal Inc., Northampton, Massachusetts) and the DASM-4 (Biopribor, Moscow [Privalov, 1980]), were used in collecting the data. All scans were obtained at a rate of 1 K min^{-1}. In all cases the reference cell was filled with the corresponding dialysate. Baseline scans were obtained with both the sample and reference cells filled with the dialysate.

NMR

NMR samples were prepared in deuterated acetate buffer and 99.9% D_2O (Aldrich). The sample used in the low salt and calcium experiment was 2.9 mM ACP, 48 mM deuterated sodium acetate (Sigma), pH 6.3. For the spectra collected in the presence of Ca^{2+}, calcium chloride was added to a final concentration of 10 mM. The sample used for the high ionic strength experiment was 3.9 mM ACP, 240 mM deuterated sodium acetate. A small amount of DTT (Boehringer-Mannheim) was added to all samples to maintain the ACP in its reduced, monomeric form.

Spectra were obtained using a GE W500 NMR spectrometer. All experiments reported are simple 1D spectra acquired using a 7-μs 90° pulse and an additional 1.0-s recycling delay to minimize errors due to incomplete relaxation. Spectra were collected at 5 °C intervals from 10 to 85 °C after thermal equilibrium was achieved. Due to the temperature dependence of the water chemical shift, an internal dioxane reference at 4.0 ppm was used for all spectra. The NMR software program Felix (Hare Research, Bothell, Washington) was used to analyze the NMR data. Lines were fit using Lorentzian lines separated by known coupling constants when appropriate. Line widths and intensities were varied using a simulated annealing algorithm to optimize fits.

Acknowledgments

We thank Dr. John E. Cronan for supplying the initial ACP gene and Blake Hill for developing the cell line for overexpression of the *E. coli* ACP gene. Dr. James Thomson's help with the calorimetry calculations is also much appreciated. This work was supported by NIH grants GM 32243 (J.H.P.) and GM 04725 (J.M.S.) and NSF grant DMB-8810329 (J.M.S.).

References

Carrington A, McLachlan AD. 1978. *Introduction to magnetic resonance*. New York: Wiley.

Connelly P, Ghosiani L, Hu CQ, Kitamura S, Tanaka A, Sturtevant JM. 1991. A differential scanning calorimetric study of the thermal unfolding of seven mutant forms of phage T4 lysozyme. *Biochemistry 30*:1887–1891.

Frederick A, Kay L, Prestegard J. 1988. Location of divalent ion sites in acyl carrier protein using relaxation perturbed 2D NMR. *FEBS Lett 238*:43–48.

Holak TA, Kearsley SK, Kim Y, Prestegard JH. 1987. Three-dimensional structure of acyl carrier protein determined by NMR pseudoenergy and distance geometry calculations. *Biochemistry 27*:6135–6142.

Kim Y, Prestegard JH. 1989. A dynamic model for the structure of acyl carrier protein in solution. *Biochemistry 28*:8792–8797.

Kim Y, Prestegard JH. 1990. Refinement of the NMR structures of acyl carrier protein with scalar coupling data. *Proteins Struct Funct Genet 8*:377–385.

Prescott DJ, Vagelos PR. 1972. Acyl carrier protein. *Methods Enzymol 36*:269–311.

Privalov PL. 1980. Scanning microcalorimeters for studying macromolecules. *Pure Appl Chem 52*:479–497.

Privalov PL, Gill SJ. 1988. Stability of protein structure and hydrophobic interactions. *Adv Protein Chem 39*:193–232.

Rock CO, Cronan JE. 1980. Improved purification of acyl carrier protein. *Anal Biochem 102*:362–364.

Roder H. 1989. Structural characterization of protein folding intermediates by proton magnetic resonance and hydrogen exchange. *Methods Enzymol 176*:446–473.

Sambrook J, Fritsch EF, Maniatis T. 1989. *Molecular cloning*. Plainview, New York: Cold Spring Harbor Laboratory Press.

Shulz H. 1977. Increased conformational stability in the presence of divalent cations. *FEBS Lett 78*:303–306.

Sturtevant JM. 1987. Biochemical applications of differential scanning calorimetry. *Annu Rev Phys Chem 38*:463–488.

Tener DM, Mayo KH. 1989. Divalent cation binding to reduced and octanoyl acyl-carrier protein. *Eur J Biochem 189*:559–565.